Effects of dynamic loading on solute transport through the human cartilage endplate

Sara L. Sampson, Meghan Sylvia, Aaron J. Fields

PII: S0021-9290(18)30892-3
DOI: https://doi.org/10.1016/j.jbiomech.2018.12.004
Reference: BM 8964

To appear in: *Journal of Biomechanics*

Received Date: 21 July 2018
Revised Date: 7 November 2018
Accepted Date: 3 December 2018

Please cite this article as: S.L. Sampson, M. Sylvia, A.J. Fields, Effects of dynamic loading on solute transport through the human cartilage endplate, *Journal of Biomechanics* (2018), doi: https://doi.org/10.1016/j.jbiomech.2018.12.004

Effects of dynamic loading on solute transport through the human cartilage endplate

Sara L. Sampson, Meghan Sylvia, Aaron J. Fields

Department of Orthopaedic Surgery, University of California, San Francisco, CA, United States

Keywords: cartilage endplate, intervertebral disc degeneration, spine, dynamic loading, biotransport

Ms. No. BM-D-18-00730R1

Original Article

Word count: 3422 (Introduction – Discussion), 3450 (Introduction – Acknowledgements)

Number of figures: 5 (plus 3 supplemental figures)

Number of tables: 3

Address for correspondence:

Aaron J. Fields, Ph.D.

513 Parnassus Avenue, S-1161 Box 0514

San Francisco, CA 94143-0514

Tel: + 1 (415) 476-0960

Fax: + 1 (415) 476-1128

aaron.fields@ucsf.edu

ABSTRACT

Nutrient and metabolite transport through the cartilage endplate (CEP) is important for maintaining proper disc nutrition, but the mechanisms of solute transport remain unclear. One unresolved issue is the role of dynamic loading. In comparison to static loading, dynamic loading is thought to enhance transport by increasing convection. However, the CEP has a high resistance to fluid flow, which could limit solute convection. Here we measure solute transport through site-matched cadaveric human lumbar CEP tissues under static *vs.* dynamic loading, and we determine how the degree of transport enhancement from dynamic loading depends on CEP porosity and solute size. We found that dynamic loading significantly increased small and large solute transport through the CEP: on average, dynamic loading increased the transport of sodium fluorescein (376 Da) by a factor of 1.85±0.64 and the transport of a large dextran (4,000 Da) by a factor of 4.97±3.05. Importantly, CEP porosity (0.65±0.07; range: 0.47-0.76) strongly influenced the degree of transport enhancement. Specifically, for both solutes, transport enhancement was greater for CEPs with low porosity than for CEPs with high porosity. This is because the CEPs with low porosity were susceptible to larger improvements in fluid flow under dynamic loading. The CEP becomes less porous and less hydrated with aging and as disc degeneration progresses. Together, these findings suggest that as those changes occur, dynamic loading has a greater effect on solute transport through the CEP compared to static loading, and thus may play a larger role in disc nutrition.

1. INTRODUCTION

Low back pain is the leading cause of disability and is closely linked to disc degeneration. Although the onset and progression of degeneration are multifactorial (Buckwalter, 1995), poor disc nutrition is believed to be a key etiologic factor (Urban et al., 2004) as well as a major obstacle that limits the capacity for regeneration (Huang et al., 2014). Due to the avascular structure of the disc, poor nutrition arises from inadequate nutrient and metabolite exchange between the disc and its surrounding tissues. Since the main pathway for entering nutrients and exiting metabolites is through the cartilage endplate (CEP) (Maroudas et al., 1975; Nachemson et al., 1970; Ohshima et al., 1989; Urban et al., 1977), understanding the mechanisms of solute transport through the CEP may provide insight into disc degeneration etiology and inform strategies for enhancing transport to slow or reverse degeneration.

The mechanisms of solute transport through the CEP remain unclear. One unresolved issue is the role of dynamic loading. In comparison to static loading, dynamic loading is thought to enhance transport by increasing convection (Schmidt et al., 2013; Zhu et al., 2012). However, the CEP has a high resistance to fluid flow (DeLucca et al., 2016; Rodriguez et al., 2011), which could limit convection. Furthermore, the effects of dynamic loading compared to static loading could depend on the porosity of the extracellular matrix. For example, when the CEP matrix is highly porous, solutes penetrate and diffuse within the matrix more freely (Roberts et al., 1996; Wu et al., 2016), and thus, dynamic loading may have a relatively small effect on transport. In contrast, reductions in CEP porosity, which occur due to changes in biosynthesis (Antoniou et al., 1996) and coincide with increased calcification (Benneker et al., 2005), could impair diffusion (Grant et al., 2016). In those cases, dynamic loading may have a larger effect.

To understand the role of dynamic loading, prior studies compared small solute transport in animal discs between static and dynamic loading conditions. An early study using dogs found that dynamic loading from moderate exercise had an insignificant effect on net transport into the disc after 2 hours (Urban et al., 1982). Similarly, dynamic flexion/extension of rabbit spines revealed an insignificant effect on solute uptake into the disc after 1 hour (Katz et al., 1986). A more recent study using rabbits indicated that low-rate dynamic loading enhanced transport into the disc at 5 minutes (Gullbrand et al., 2015), but

the net effect (16.8% *vs.* unloaded controls) was relatively modest. However, those animals have healthy CEPs with porosities (~0.70 to 0.80) at the upper end of the range seen in adult humans (0.43 to 0.74) (Wu et al., 2016), and thus, the effects of low CEP porosity on transport enhancement are unclear. Likewise, because convection depends on solute size (Albro et al., 2011; Ferguson et al., 2004), the relative influence of CEP porosity versus solute size also remains unknown. To address this, we measured the effects of dynamic loading on solute transport through the human CEP, and we determined how any transport enhancement from dynamic loading depends on CEP porosity and solute size.

2. METHODS

2.1 CEP sample preparation

Nine fresh cadaveric lumbar spines (age range: 38 to 73 years, mean: 60.8 years) were obtained from donors with no medical history of musculoskeletal disorders (UCSF Willed Body Program). Intact CEPs, including any calcified cartilage, were lifted from the subchondral bone and trimmed of nucleus pulposus tissue with a razor blade, using the relative difference in transparency between the nucleus tissue and CEP as a guide (Wu et al., 2016). All CEP samples were taken from the central region adjacent to the nucleus pulposus. For every level and donor, the harvested CEP tissues were prepared into site-matched pairs, using a biopsy punch (4 mm-diameter), which resulted in 46 CEP samples (**Table 1**). In this way, each sample tested under dynamic loading was compared to a donor-, level-, and site-matched control sample tested under static loading conditions.

2.2 Solute transport measurements

2.2.1 Static and dynamic loading

Since nucleus pressure compacts the CEP and leads to smaller pore size and lower permeability (Ayotte et al., 2001; Dhillon et al., 2001), we used a permeation test with a custom loading apparatus (**Fig. 1**) to model this *in situ* condition. This allowed us to precisely control the driving hydraulic pressure against the CEP to match physiologic disc pressures. The upstream inlet of the sample holder connected to a reservoir containing fluorescently labeled solutes ($C_{upstream}$ = 0.27 mM in PBS). The solute reservoir

was affixed in-line with the actuator of an ElectroForce 3200 load frame (TA Instruments, Eden Prairie, MN), which pressurized the solution by depressing a piston. Fluid and solutes passed through the CEP and were collected in a chamber downstream containing 7 mL of PBS. For static loading experiments, we used a pressure magnitude (0.6 MPa) that is in the upper end of the intradiscal pressure range measured during various static sitting postures (Nachemson, 1966; Wilke et al., 1999); for dynamic loading experiments, we applied a pressure range (0.6-1.0 MPa) and sinusoidal frequency (0.5 Hz) similar to those measured in the disc during stairclimbing (Wilke et al., 1999). In each test, fluid pressures were maintained by adjusting the piston position using feedback from a load cell (Honeywell Sensotec; Columbus, Ohio, Model 11; Appendix A). All loading experiments were 80 minutes in duration, since pilot studies conducted to 120 minutes showed that increases in the downstream concentration beyond 80 minutes were only about ~3-4%.

2.2.2 Flow rate estimates

During the loading experiments, the control software (WinTest 4.1; TA Instruments) continuously increased the piston displacement to maintain the prescribed loads. These continuous piston adjustments compensated for the load loss that would otherwise have occurred as fluid flowed through the CEP (Appendix A). Thus, the total change in piston displacement (Δd_{piston}) over the course of the 80-minute test (Δt) was used to estimate the average volumetric flow rate (Q) through the CEP according to the relation $Q = \Delta d_{piston} * A_{piston} / \Delta t$, where A_{piston} is the cross-sectional area of the piston (12.7 mm-diameter).

2.2.3 Fluorescently labeled solutes

To determine the effect of solute size, we conducted experiments with two solutes: a 376 Da-sized sodium fluorescein salt ($C_{upstream}$ = 0.1 mg/mL, F3677 Sigma-Aldrich, St. Louis, MO) and 4,000 Da-sized fluorescein isothiocyanate (FITC)–dextran ($C_{upstream}$ = 1.1 mg/mL, 46944 Sigma-Aldrich). These solutes were chosen because they span a size range that encompasses small nutrients (glucose = 180 Da) and growth factors (5,000 to 10,000 Da).

2.2.4 Solute transport measurements

To quantify solute transport through each CEP sample, aliquots of the solution downstream from the CEP were collected at 0, 5, 10, 20, 40, and 80 minutes and assayed for solute concentration ($C_{downstream}$). Fluorescence measurements for each solute (376 Da: ex/em 460/515 nm; 4,000 Da: ex/em 494/525 nm) were acquired using a SpectraMax M5 spectrophotometer (Molecular Devices, San Jose, CA), and were referenced to a standard curve of known solute concentrations. Downstream solute concentrations were normalized to the upstream solute concentrations ($\hat{C} = C_{downstream}/C_{upstream}$) for each sample to enable comparisons of solute transport between loading conditions (static *vs.* dynamic) and solute sizes (376 Da *vs.* 4,000 Da). To determine specimen-specific transport enhancement from dynamic loading, the concentration ratio for each CEP sample under dynamic loading was normalized to the concentration ratio of its site-matched control sample under static loading ($\hat{C}_{dynamic}/\hat{C}_{static}$).

2.3 CEP biochemical composition and structure

2.3.1 Porosity and hydration

After loading, CEP porosity (ϕ^w) was determined using the buoyancy technique (Gu et al., 1996, 2004), which gives an estimate of the fluid volume fraction:

$$\phi^w = V_w / V_{total} = \frac{weight_{wet} - weight_{dry}}{weight_{wet} - weight_{pbs}} \frac{\rho_{pbs}}{\rho_w}$$

The dry weight ($weight_{dry}$), wet weight in air ($weight_{wet}$) and the weight in PBS ($weight_{pbs}$) were measured using a semi-micro analytical balance fitted with a density kit. CEP hydration, i.e. ($weight_{wet} - weight_{dry}$)/$weight_{dry}$, was also calculated (Appendix B).

2.3.2 Biochemical composition

Sulfated glycosaminoglycan (*s*-GAG) and collagen contents were determined using dimethylmethylene blue and chloramine-T assays (Appendix B), according to previous methods (Farndale et al., 1986; Fields et al., 2014; Woessner, 1961).

2.3.3 CEP thickness

Prior to testing, the thickness of the CEP samples was measured with a micrometer designed to sense the tissue's electrical conductivity (Fields et al., 2014).

2.4 Statistical Analysis

We used a two-way ANOVA to evaluate differences in CEP characteristics between samples tested with different loading conditions and with different solutes. Un-paired two-tailed *t*-tests were used to compare the average concentration ratios for static and dynamic loading at each time point. Additionally, Pearson's correlation coefficients were used to analyze the role of CEP characteristics in transport enhancement that was determined at the end of the experiments. Un-paired *t*-tests were used to compare transport enhancement between samples tested with different solutes. All statistical analyses were performed using JMP Pro 14 (SAS Institute; Cary, NC). A p-value < 0.05 was considered statistically significant. Data are given as mean ± SD.

3. RESULTS

Average compositional traits were similar for the statically and dynamically loaded samples tested with a given solute (**Table 2**). Average CEP porosity was 0.648±0.069 (0.47 to 0.76), which is typical of CEP tissues from 40-70 year-olds and is within the range of previously reported values (Wu et al., 2016). Likewise, average collagen content (681±171 µg/mg dry weight), average *s*-GAG content (103±31 µg/mg dry weight) and average CEP thickness (0.676±0.351 mm) were also within their respective ranges for human lumbar CEP tissues (Berg-Johansen et al., 2018; Fields et al., 2015, 2014; Roberts et al., 1989).

Analysis of the normalized concentration ratios ($C_{downstream}/C_{upstream}$) indicated that dynamic loading increased solute transport for each CEP sample compared to its site-matched control tested under static loading conditions. However, on average, the group differences in concentration ratios between statically and dynamically loaded samples were not statistically significant for the 376-Da solute because of the large heterogeneity in transport within each group (p = 0.306-0.880; **Fig. 2A**). For the 4,000-Da solute, average concentration ratios from dynamic loading were significantly higher at 20 min and 40 min (p = 0.048; **Fig. 2B**). For both loading conditions, average concentration ratios were significantly lower for the 4,000-Da solute than the 376-Da solute at the end of loading (static: p = 0.045; dynamic p = 0.016).

To investigate CEP-specific factors that influence the relative amount of solute transport under dynamic *vs.* static loading, final transport enhancement from dynamic loading was calculated for each site-matched pair, and variations in transport enhancement amongst the pairs were related to the average structural and biochemical characteristics for each pair. Results showed that the degree to which dynamic loading enhanced solute transport depended on solute size and was most strongly correlated with CEP porosity (**Table 3**). Specifically, final transport enhancement ratios ($\hat{C}_{dynamic}/\hat{C}_{static}$) ranged from 1.07-2.67 for the 376-Da solute and 2.30-9.83 for the 4,000-Da solute. Importantly, for both solutes, transport enhancement was highly correlated with CEP porosity, with the greatest enhancement occurring for the least porous CEP samples (**Fig. 3**). Furthermore, in the CEP samples with low porosities, the transport enhancement was notably higher for the 4,000-Da solute than the 376-Da solute, although the difference was smaller for higher porosity values (**Fig. 3**). On average, transport enhancement for the 4,000-Da solute was 2.7-fold greater than the 376-Da solute (4.97±3.05 *vs.* 1.85±0.64, $p < 0.002$).

Transport enhancement for both solutes was also independently correlated with CEP hydration (376 Da: $r = -0.905$, $p < 0.0001$; 4,000 Da: $r = -0.865$, $p < 0.01$). This finding reflected the strong positive relationship between CEP hydration and porosity (**Fig. 4**). For the 376-Da solute, transport enhancement was also significantly greater for CEPs with lower *s*-GAG content (**Table 3**). Neither collagen content nor thickness was independently associated with transport enhancement for either solute.

In general, downstream concentrations increased rapidly during the first 20 minutes and then plateaued (**Fig. 5**), reaching final concentrations that were 0.001% to 0.01% of upstream values. For CEP samples with the highest porosities, solute penetration under static loading occurred readily (**Fig. 5A**), and thus, dynamic loading led to only small-to-modest transport improvements (376 Da: $\hat{C}_{dynamic}/\hat{C}_{static} = 1.07$; 4,000 Da: $\hat{C}_{dynamic}/\hat{C}_{static} = 2.30$). In contrast, for CEPs with the lowest porosities, solute penetration under static loading was poor, and thus, the final downstream concentrations only reached low values (**Fig. 5B**). In those cases, dynamic loading led to greater improvements in transport (376 Da: $\hat{C}_{dynamic}/\hat{C}_{static} = 2.67$; 4,000 Da: $\hat{C}_{dynamic}/\hat{C}_{static} = 9.83$). These observations were supported by fluid flow estimates, which showed large increases in flow under dynamic loading (**Fig. 5C**).

4. DISCUSSION

We measured the effects of dynamic loading on small and large solute transport through human cadaveric CEP tissues, and we determined how the degree of transport enhancement from dynamic loading depends on CEP porosity and solute size. On an individual basis, dynamic loading significantly increased transport through each CEP sample compared to its statically-loaded, site-matched control. However, on average, the effects of dynamic loading were obscured by CEP-specific characteristics. To investigate these characteristics, we analyzed the transport enhancement values for site-matched CEP samples (**Table 3**). One important characteristic that strongly influenced the degree of transport enhancement was CEP porosity, which ranged from 0.47-0.76. Specifically, for both solute sizes, transport enhancement was greater for CEPs with low porosities than for CEPs with high porosities (**Fig. 3**). This is because the CEPs with low porosities were susceptible to large improvements in fluid flow under dynamic loading (**Fig. 5C**). Moreover, the transport enhancement from dynamic loading had a greater effect on the 4,000-Da solute than the 376-Da solute: dynamic loading significantly increased 376 Da-fluorescein transport by up to 2.67-fold compared to static loading and 4,000 Da-dextran transport by up to 9.83-fold. Transport of the larger solute through the CEP occurred relatively slowly under static load (**Fig. 2B**), especially in cases where CEP porosity was low (**Fig. 5B**). The CEP is an important gateway for nutrient and metabolite exchange between the nucleus pulposus and vertebral capillaries. Prior work indicates that the CEP becomes less porous (Grant et al., 2016), less hydrated (Antoniou et al., 1996; Maroudas et al., 1975), and less permeable (DeLucca et al., 2016) with aging and as disc degeneration progresses. Taken together, our results suggest that as those changes occur, dynamic loading has a greater effect on solute transport through the CEP compared to static loading, and thus, dynamic loading may play a larger role in disc nutrition.

Our experiments reveal that the degree to which dynamic loading improves solute transport compared to static loading depends on matrix porosity and hydration. Prior studies found that dynamic loading had an insignificant effect on small molecule transport into the disc in adult dogs (Urban et al., 1982) and

rabbits (Katz et al., 1986), which have healthy discs and CEP tissues. The present findings similarly indicated that when CEP porosity was high, small solute transport under static loading was appreciable, and thus, dynamic loading led to relatively small transport enhancement (average $\hat{C}_{dynamic}/\hat{C}_{static}$ = 1.25 for CEPs with $\phi^w \geq 0.70$). However, when the CEP was less porous, we found that dynamic loading greatly increased small molecule transport (average $\hat{C}_{dynamic}/\hat{C}_{static}$ = 2.63 for CEPs with $\phi^w \leq 0.60$). In those cases, fluid flow under static loading was relatively low, but increased dramatically with dynamic loading ($Q_{dynamic}/Q_{static}$ = 18.5 for ϕ^w = 0.55, $Q_{dynamic}/Q_{static}$ = 11.3 for ϕ^w = 0.74). To understand the importance of fluid flow in those cases, we estimated Peclet (*Pe*) numbers according to the relationship $Pe = {}^{UL}/_{D}$ (Jackson and Gu, 2009), where *U* is the fluid velocity, *L* is the CEP thickness, and *D* is the solute diffusivity (Appendix C). If *Pe* > 1, convection dominates transport, whereas for *Pe* < 1, diffusion is more important. For the smaller solute under static loading, estimated Peclet numbers ranged between 3.28-4.83 (3.90±0.74); for dynamic loading between 46.41-74.98 (70.35±19.47). This suggests that dynamic loading improves solute transport by enhancing convective transport, and that convection may be the dominant mode of transport, even under static loading of this magnitude. On the basis of these findings, it appears reasonable to hypothesize that convective transport has a considerable impact on disc nutrition. These results also motivate future studies of disc nutrition to consider high and low CEP porosities, especially when studying the effects of aging or disc degeneration.

The relative effects of dynamic loading on transport also depended on solute size. The 4,000-Da solute showed greater increases in transport from dynamic loading than the 376-Da solute. This finding may be explained by results from previous studies, which showed that larger solutes have lower partition coefficients in the CEP, and thus, they enter and permeate within the matrix to a lesser extent than the smaller solutes (Roberts et al., 1996). Consequently, the larger solutes benefit more from convective transport (Ferguson et al., 2004; Gantenbein et al., 2006; O'Hara et al., 1990). Although the results from the fluorescein experiments are most relevant to small nutrients and metabolites and the 4,000 Da-dextran is similar in size to small growth factors, it is worth noting that the dextran has a linear molecular

structure, which can affect transport independently of size. Specifically, the linear structures can readily bend, allowing them to move more easily through a tortuous cartilage matrix in comparison to globular or spherical solutes of the same molecular weight (DiDomenico et al., 2018). In comparing the transport data between the two solutes, it is also worth noting that CEP samples in the 4,000-Da group were 38% thinner than those in the 376-Da group ($p < 0.05$; **Table 2**). Although there was no significant correlation between CEP thickness and transport enhancement for either solute in the range of thicknesses respectively tested (**Table 3**), it is possible that testing thicker CEP samples with the 4,000-Da solute would slow its transport, thereby accentuating the differences in transport and transport enhancement between the two solutes.

One limitation of the study is that we removed the CEP from the bony endplate, and this could alter the transport properties. For example, compaction of the CEP against the bony endplate could decrease the pore space and thereby lower permeability (Ayotte et al., 2001). Using our flow rate estimates and Darcy's law, we estimate that the statically loaded CEPs had an average hydraulic permeability of $1.27 \times 10^{-16} \pm 0.49 \times 10^{-16}$ m^4/Ns, which is similar to human CEP permeability determined in confined compression ($1.62 \times 10^{-16} \pm 1.08 \times 10^{-16}$ m^4/Ns for CEP samples from Pfirrmann grade 3 discs) (DeLucca et al., 2016). This suggests that any effects of removing the CEP from the bone were small. Moreover, CEP permeability is an order of magnitude lower than bony endplate permeability, and accordingly, the net permeability of the two combined is more highly correlated with the cartilage component ($r^2 = 0.96$; $p < 0.0001$) than with the bony component ($r^2 = 0.08$, $p = 0.06$) (Rodriguez et al., 2011). Thus, we expect that retaining the bone would not change our overall conclusions.

It is also appreciated that the effects of dynamic loading on solute transport depend on solute charge (Gu et al., 2004) and loading magnitude/frequency (DiDomenico et al., 2016). Additional testing showed that using a higher static pressure (1.0 MPa) increased the fluid flow rate compared to the original protocol with lower static pressure (0.6 MPa static: $4.7 \times 10^{-13} \pm 2.4 \times 10^{-13}$ m^3/s; 1.0 MPa static: $9.7 \times 10^{-13} \pm 4.3 \times 10^{-13}$ m^3/s; see Appendix D). However, the corresponding decrease in transport enhancement from dynamic loading was just 4.6% on average ($p = 0.75$). Part of the reason for this small effect is that

the increase in transport with the higher static load was relatively small compared to the increase from dynamic loading. Thus, while any estimates of transport enhancement likely depend on the relative magnitudes of static *vs.* dynamic pressures, these findings suggest that for our prescribed loading conditions, the pressure magnitude effect was small relative to the dynamic effect. Clearly, additional studies with human CEP tissues are needed to address different pressure magnitudes, loading frequencies, and solute charges.

In summary, our findings reveal that dynamic loading enhances small and large solute transport through the human CEP compared to static loading, and that the degree of transport enhancement is greater for CEPs with low porosities and for larger solutes. We conclude that dynamic loading may play a consequential role in disc nutrition, although the effectiveness of dynamic loading as a strategy for improving disc nutrition is likely to depend on patient-specific factors such as CEP porosity. Furthermore, the present relationships may be useful in developing more physiologic computational models of disc nutrition and for guiding the design of replacement tissues with improved transport characteristics.

ACKNOWLEDGEMENTS

This study was supported by the North American Spine Society, the UCSF School of Medicine Research Allocation Committee, and the National Institutes of Health (P30AR066262 and R01AR070198).

CONFLICT OF INTEREST STATEMENT

None of the authors report any conflicts of interest.

REFERENCES

Albro, M.B., Banerjee, R.E., Li, R., Oungoulian, S.R., Chen, B., del Palomar, A.P., Hung, C.T., Ateshian, G.A., 2011. Dynamic loading of immature epiphyseal cartilage pumps nutrients out of vascular canals. J. Biomech. 44, 1654–1659. https://doi.org/10.1016/j.jbiomech.2011.03.026

Antoniou, J., Goudsouzian, N.M., Heathfield, T.F., Winterbottom, N., Steffen, T., Poole, A.R., Aebi, M., Alini, M., 1996. The Human Lumbar Endplate. Spine (Phila. Pa. 1976). 21, 1153–1161. https://doi.org/10.1097/00007632-199605150-00006

Ayotte, D.C., Ito, K., Tepic, S., 2001. Direction-dependent resistance to flow in the endplate of the intervertebral disc: an ex vivo study. J. Orthop. Res. 19, 1073–1077. https://doi.org/10.1016/S0736-0266(01)00038-9

Benneker, L.M., Heini, P.F., Alini, M., Anderson, S.E., Ito, K., 2005. 2004 Young Investigator Award Winner: Vertebral Endplate Marrow Contact Channel Occlusions and Intervertebral Disc Degeneration. Spine (Phila. Pa. 1976). 30, 167–173. https://doi.org/10.1097/01.brs.0000150833.93248.09

Berg-Johansen, B., Han, M., Fields, A.J., Liebenberg, E.C., Lim, B.J., Larson, P.E., Gunduz-Demir, C., Kazakia, G.J., Krug, R., Lotz, J.C., 2018. Cartilage Endplate Thickness Variation Measured by Ultrashort Echo-Time MRI Is Associated With Adjacent Disc Degeneration. Spine (Phila. Pa. 1976). 43, E592–E600. https://doi.org/10.1097/BRS.0000000000002432

Buckwalter, J.A., 1995. Aging and degeneration of the human intervertebral disc. Spine (Phila. Pa. 1976). 20, 1307–14.

DeLucca, J.F., Cortes, D.H., Jacobs, N.T., Vresilovic, E.J., Duncan, R.L., Elliott, D.M., 2016. Human cartilage endplate permeability varies with degeneration and intervertebral disc site. J. Biomech. 49, 550–557. https://doi.org/10.1016/j.jbiomech.2016.01.007

Dhillon, N., Bass, E.C., Lotz, J.C., 2001. Effect of Frozen Storage on the Creep Behavior of Human Intervertebral Discs. Spine (Phila. Pa. 1976). 26, 883–888. https://doi.org/10.1097/00007632-200104150-00011

DiDomenico, C.D., Lintz, M., Bonassar, L.J., 2018. Molecular transport in articular cartilage — what have we learned from the past 50 years? Nat. Rev. Rheumatol. 14, 393–403. https://doi.org/10.1038/s41584-018-0033-5

DiDomenico, C.D., Xiang Wang, Z., Bonassar, L.J., 2016. Cyclic Mechanical Loading Enhances Transport of Antibodies Into Articular Cartilage. J. Biomech. Eng. 139, 011012. https://doi.org/10.1115/1.4035265

Farndale, R.W., Buttle, D.J., Barrett, A.J., 1986. Improved quantitation and discrimination of sulphated glycosaminoglycans by use of dimethylmethylene blue. Biochim. Biophys. Acta 883, 173–7. https://doi.org/10.1016/0304-4165(86)90306-5

Ferguson, S.J., Ito, K., Nolte, L.-P., 2004. Fluid flow and convective transport of solutes within the intervertebral disc. J. Biomech. 37, 213–221. https://doi.org/10.1016/S0021-9290(03)00250-1

Fields, A.J., Han, M., Krug, R., Lotz, J.C., 2015. Cartilaginous end plates: Quantitative MR imaging with very short echo times-orientation dependence and correlation with biochemical composition. Radiology 274, 482–9. https://doi.org/10.1148/radiol.14141082

Fields, A.J., Rodriguez, D., Gary, K.N., Liebenberg, E.C., Lotz, J.C., 2014. Influence of biochemical composition on endplate cartilage tensile properties in the human lumbar spine. J. Orthop. Res. 32, 245–252. https://doi.org/10.1002/jor.22516

Gantenbein, B., Grünhagen, T., Lee, C.R., van Donkelaar, C.C., Alini, M., Ito, K., 2006. An In Vitro Organ Culturing System for Intervertebral Disc Explants With Vertebral Endplates. Spine (Phila. Pa. 1976). 31, 2665–2673. https://doi.org/10.1097/01.brs.0000244620.15386.df

Grant, M., Epure, L., Bokhari, R., Roughley, P., Antoniou, J., Mwale, F., 2016. Human cartilaginous endplate degeneration is induced by calcium and the extracellular calcium-sensing receptor in the intervertebral disc. Eur. Cells Mater. 32, 137–151. https://doi.org/10.22203/eCM.v032a09

Gu, W., Lewis, B., Lai, W.M., Ratcliffe, A., Mow, V.C., 1996. A Technique for measuring volume and true density of the solid matrix of cartilaginous tissues, in: Advances in Bioengineering, American Society of Mechanical Engineers, Bioengineering Division (Publication) BED. pp. 89–90.

Gu, W.Y., Yao, H., Vega, A.L., Flagler, D., 2004. Diffusivity of Ions in Agarose Gels and Intervertebral Disc: Effect of Porosity. Ann. Biomed. Eng. 32, 1710–1717. https://doi.org/10.1007/s10439-004-7823-4

Gullbrand, S.E., Peterson, J., Ahlborn, J., Mastropolo, R., Fricker, A., Roberts, T.T., Abousayed, M., Lawrence, J.P., Glennon, J.C., Ledet, E.H., 2015. ISSLS Prize Winner. Spine (Phila. Pa. 1976). 40, 1158–1164. https://doi.org/10.1097/BRS.0000000000001012

Huang, Y.-C., Urban, J.P.G., Luk, K.D.K., 2014. Intervertebral disc regeneration: do nutrients lead the way? Nat. Rev. Rheumatol. 10, 561–566. https://doi.org/10.1038/nrrheum.2014.91

Jackson, A., Gu, W.Y., 2009. Transport Properties of Cartilaginous Tissues. Curr. Rheumatol. Rev. 5, 40–50. https://doi.org/10.2174/157339709787315320

Katz, M.M., Hargens, A.R., Garfin, S.R., 1986. Intervertebral disc nutrition. Diffusion versus convection. Clin. Orthop. Relat. Res. 243–5.

Maroudas, A., Stockwell, R.A., Nachemson, A., Urban, J., 1975. Factors involved in the nutrition of the human lumbar intervertebral disc: cellularity and diffusion of glucose in vitro. J. Anat. 120, 113–30.

Nachemson, A., 1966. The load on lumbar disks in different positions of the body. Clin. Orthop. Relat. Res. 45, 107–22.

Nachemson, A., Lewin, T., Maroudas, A., Freeman, M.A., 1970. In vitro diffusion of dye through the end-plates and the annulus fibrosus of human lumbar inter-vertebral discs. Acta Orthop. Scand. 41, 589–607.

O'Hara, B.P., Urban, J.P., Maroudas, A., 1990. Influence of cyclic loading on the nutrition of articular cartilage. Ann. Rheum. Dis. 49, 536–9.

Ohshima, H., Tsuji, H., Hirano, N., Ishihara, H., Katoh, Y., Yamada, H., 1989. Water diffusion pathway, swelling pressure, and biomechanical properties of the intervertebral disc during compression load. Spine (Phila. Pa. 1976). 14, 1234–44.

Roberts, S., Menage, J., Urban, J.P., 1989. Biochemical and structural properties of the cartilage end-plate and its relation to the intervertebral disc. Spine (Phila. Pa. 1976). 14, 166–74.

Roberts, S., Urban, J.P.G., Evans, H., Eisenstein, S.M., 1996. Transport Properties of the Human Cartilage Endplate in Relation to Its Composition and Calcification. Spine (Phila. Pa. 1976). 21, 415–420. https://doi.org/10.1097/00007632-199602150-00003

Rodriguez, A.G., Slichter, C.K., Acosta, F.L., Rodriguez-Soto, A.E., Burghardt, A.J., Majumdar, S., Lotz, J.C., 2011. Human Disc Nucleus Properties and Vertebral Endplate Permeability. Spine (Phila. Pa. 1976). 36, 512–520. https://doi.org/10.1097/BRS.0b013e3181f72b94

Schmidt, H., Galbusera, F., Rohlmann, A., Shirazi-Adl, A., 2013. What have we learned from finite element model studies of lumbar intervertebral discs in the past four decades? J. Biomech. 46, 2342–2355. https://doi.org/10.1016/j.jbiomech.2013.07.014

Urban, J., Holm, S., Maroudas, A., Nachemson, A., 1982. Nutrition of the intervertebral disc: effect of fluid flow on solute transport. Clin. Orthop. Relat. Res. 170, 296.

Urban, J.P., Holm, S., Maroudas, A., Nachemson, A., 1977. Nutrition of the intervertebral disk. An in vivo study of solute transport. Clin. Orthop. Relat. Res. 101—114.

Urban, J.P.G., Smith, S., Fairbank, J.C.T., 2004. Nutrition of the intervertebral disc. Spine (Phila. Pa. 1976). 29, 2700–2709.

Wilke, H.J., Neef, P., Caimi, M., Hoogland, T., Claes, L.E., 1999. New in vivo measurements of pressures in the intervertebral disc in daily life. Spine (Phila. Pa. 1976). 24, 755–62. https://doi.org/10.1097/00007632-199904150-00005

Woessner, J.F., 1961. The determination of hydroxyproline in tissue and protein samples containing small proportions of this imino acid. Arch. Biochem. Biophys. 93, 440–447. https://doi.org/10.1016/0003-9861(61)90291-0

Wu, Y., Cisewski, S.E., Wegner, N., Zhao, S., Pellegrini, V.D., Slate, E.H., Yao, H., 2016. Region and strain-dependent diffusivities of glucose and lactate in healthy human cartilage endplate. J. Biomech. 49, 2756–2762. https://doi.org/10.1016/j.jbiomech.2016.06.008

Zhu, Q., Jackson, A.R., Gu, W.Y., 2012. Cell viability in intervertebral disc under various nutritional and dynamic loading conditions: 3d Finite element analysis. J. Biomech. 45, 2769–2777.

https://doi.org/10.1016/j.jbiomech.2012.08.044

Figure legends:

Figure 1. Schematic of apparatus for applying static and dynamic hydraulic pressure to the CEP. The sample holder of the loading apparatus was comprised of upper and lower plates that allow fluid flow through a 2 mm-diameter through-hole. The piston connects to the actuator of a load frame, which maintains the desired upstream pressures using feedback from a load cell.

Figure 2. Comparison of concentration ratios (mean ± SD) between static and dynamic loading at various time points during the loading experiments performed with **(A)** 376 Da solutes and **(B)** 4,000 Da solutes. * $p < 0.05$ static *vs.* dynamic unpaired *t*-test.

Figure 3. Transport enhancement correlated significantly with CEP porosity for tests using the 376 Da solute ($p < 0.0001$) and the 4,000 Da solute ($p < 0.0001$). The dashed line at $y = 1$ represents equivalent solute transport under static and dynamic loading conditions. Solute transport enhancement ($\hat{C}_{dynamic}/\hat{C}_{static}$) from dynamic loading was calculated at the end of the 80-minute loading period. The linear equation used to fit the 376 Da data is $y = -9.2x + 7.9$. An exponential curve was used to fit the 4,000 Da data because the slope of the relationship significantly decreases in magnitude at porosities above 0.65. The equation of the exponential curve shown is $y = 2450*e^{-9.995x}$.

Figure 4. CEP hydration (water content by weight) was significantly correlated ($p < 0.0001$) with CEP porosity (water content by volume).

Figure 5. Downstream concentrations increased dramatically during the first 20 minutes and then

plateaued. Final downstream concentrations were 0.001% to 0.01% of upstream concentrations. For CEPs with low porosity, solute penetration under static loading was so poor that convective pumping from dynamic loading substantially increased solute transport. **(A)** Examples of solute transport kinetics through CEPs with high porosity (ϕ^w = 0.71 with 376 Da; ϕ^w = 0.68 with 4,000 Da). **(B)** Examples of solute transport kinetics through CEPs with relatively low porosity (ϕ^w = 0.54 with 376 Da; ϕ^w = 0.59 with 4,000 Da). **(C)** Flow rate estimates were significantly correlated with CEP porosity (dynamic loading: r = 0.84, p = 0.001; static loading: r = 0.69, p = 0.018). The slowest flow rates calculated for low porosity CEPs were consistent with the low concentration ratios measured for low porosity CEPs in panel (B). On average, the flow rate was an order of magnitude faster for dynamic loading compared to static loading (6.2±2.6 x 10^{-12} m^3/s *vs.* 4.7±2.4 x 10^{-13} m^3/s, $p < 0.001$). Flow rate estimates were pooled from experiments performed with 376 Da and 4,000 Da solutes. The specimen-specific flow-rate enhancement from dynamic loading ($Q_{dynamic}/Q_{static}$) was greatest for the lowest porosity CEPs. For example, ($Q_{dynamic}/Q_{static}$ = 18.5 for ϕ^w = 0.55 and $Q_{dynamic}/Q_{static}$ = 11.3 for ϕ^w = 0.74).

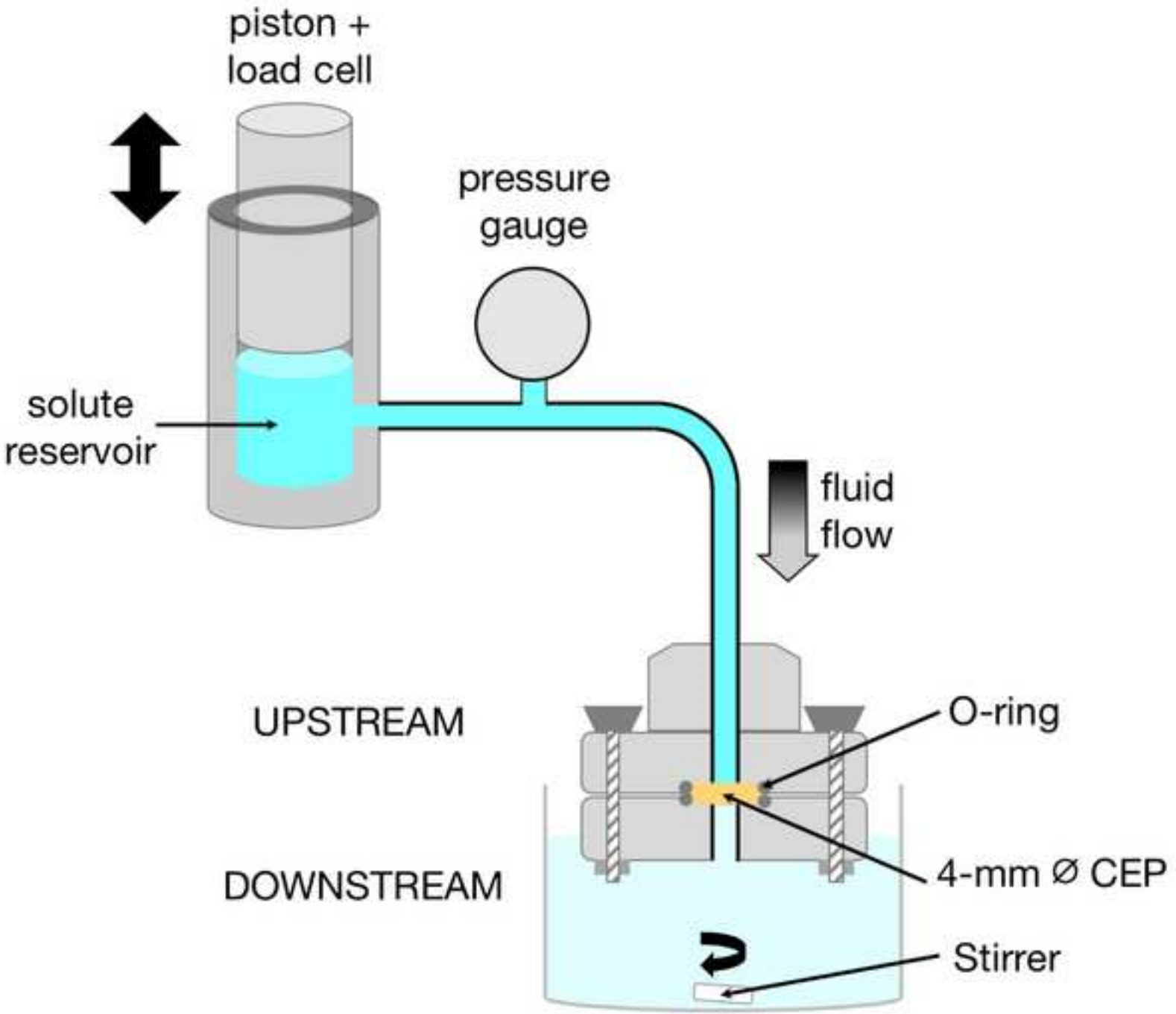
piston +
load cell
pressure
gauge
solute
reservoir
fluid
flow
UPSTREAM
O-ring
DOWNSTREAM
4-mm Ø CEP
Stirrer

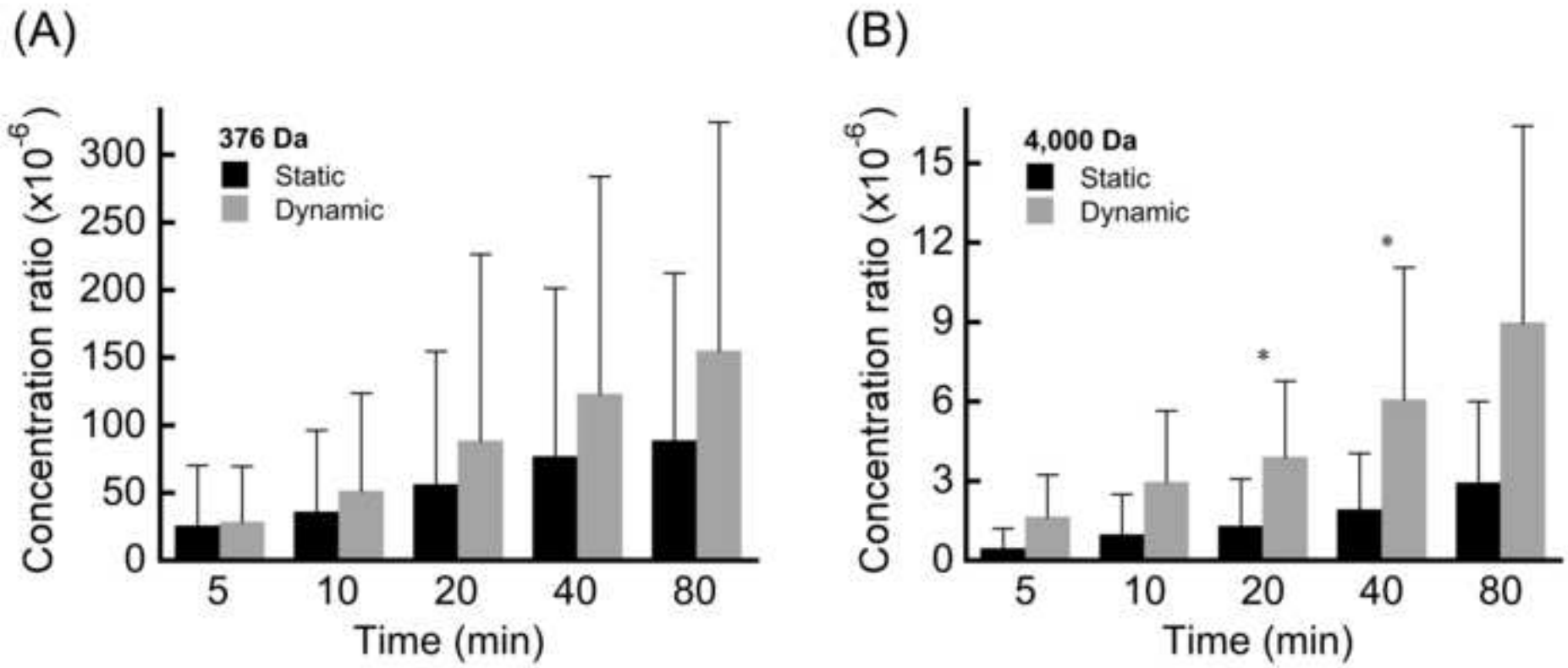

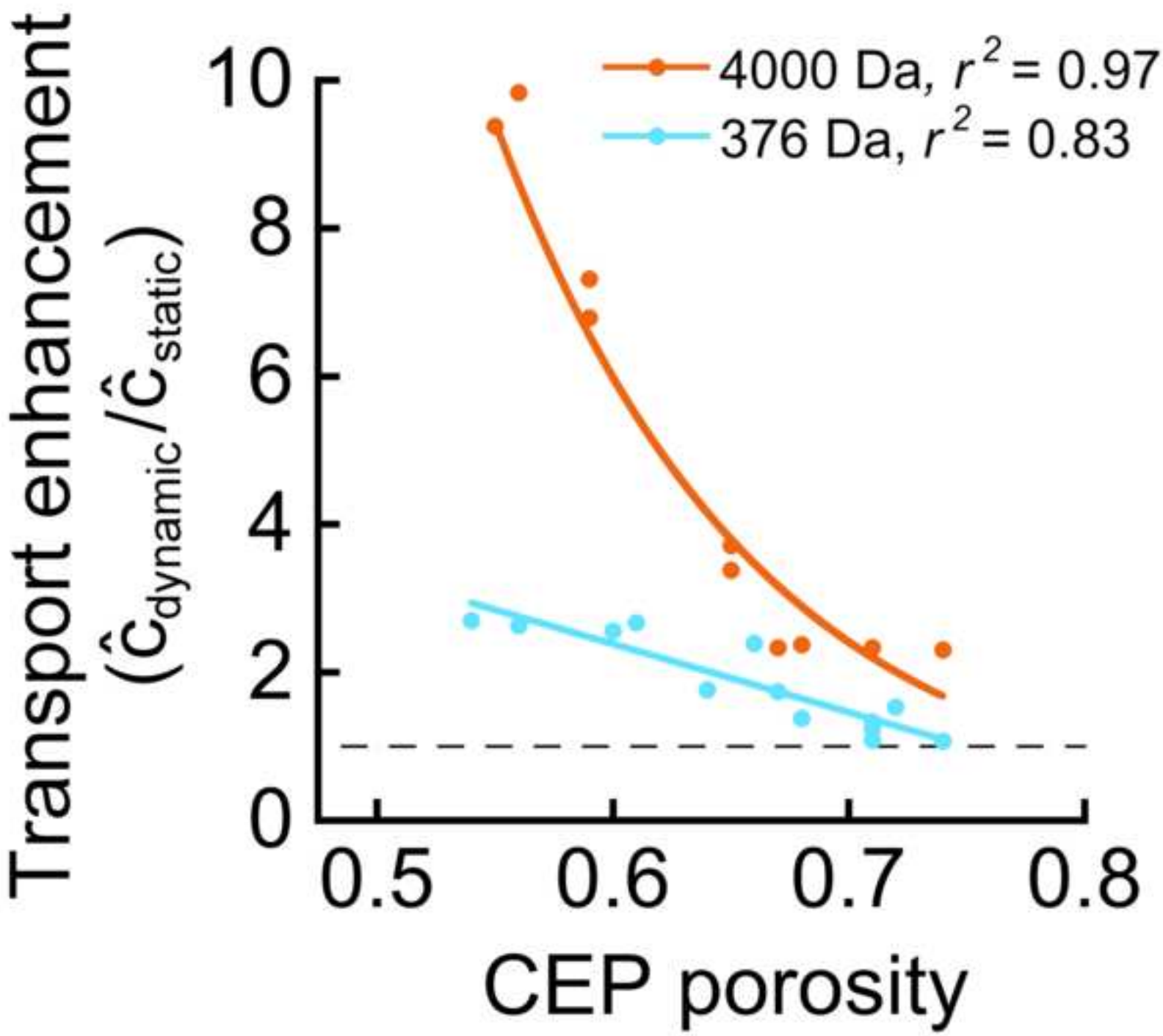

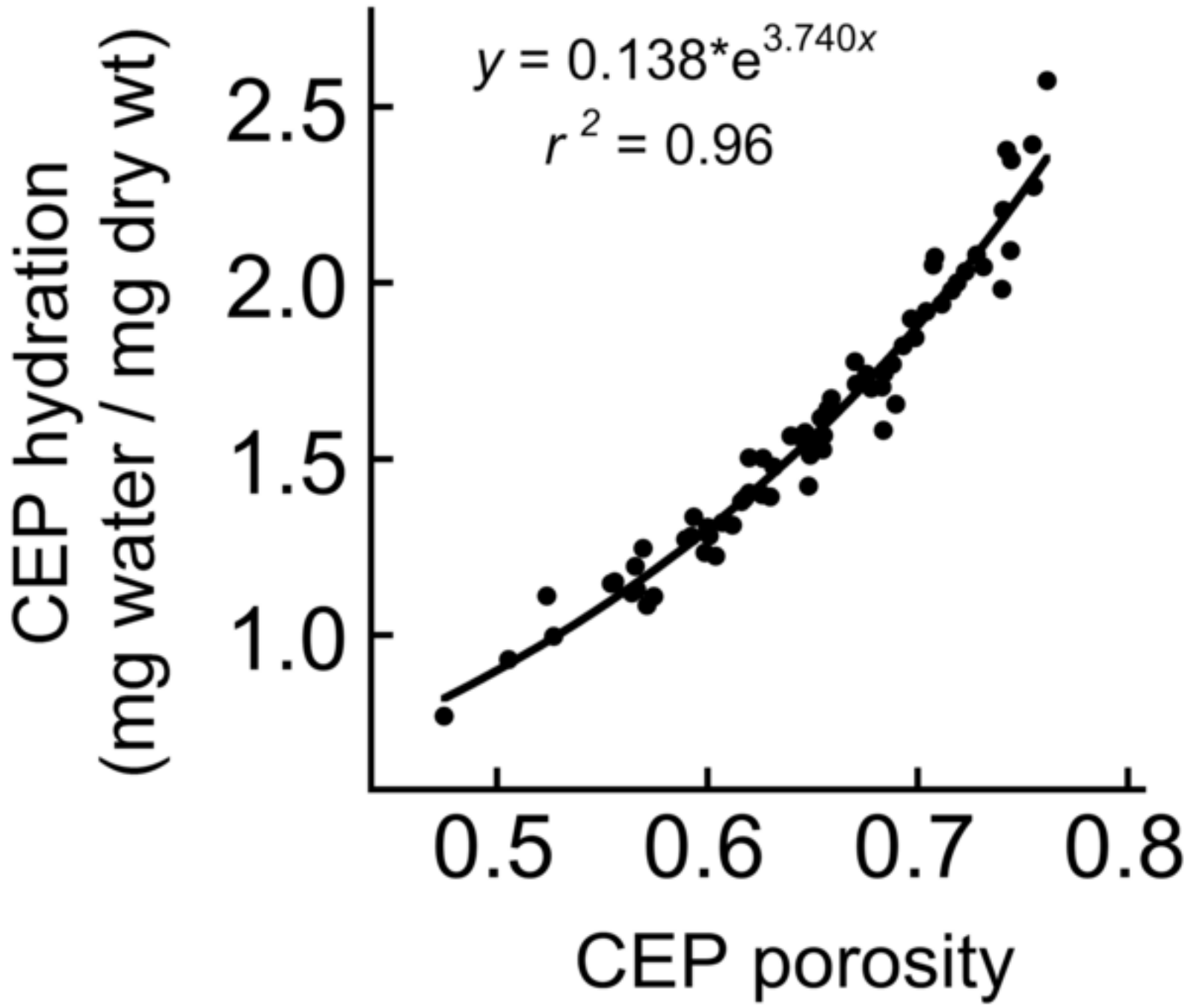

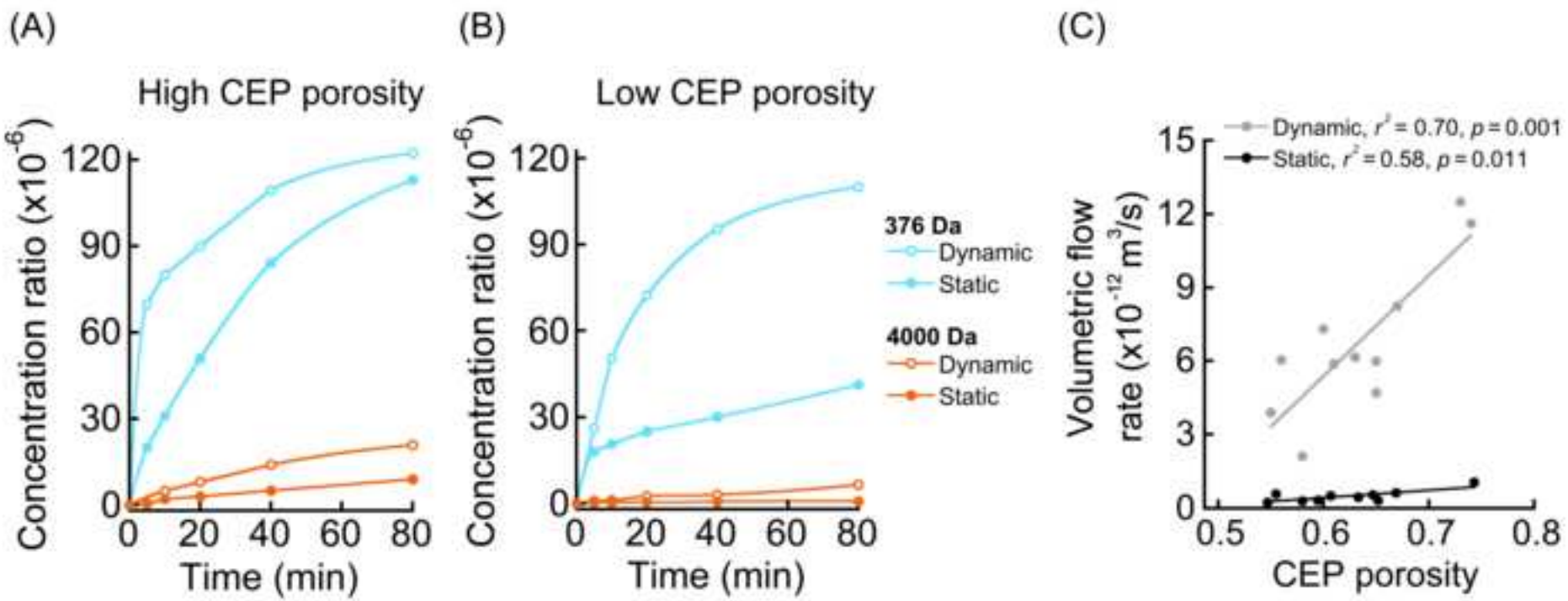

Tables:

Table 1. Number and level of 46 human lumbar CEP samples used in the study.

Level		CEP samples (*n*)	Spines
L1-L2	superior	6	3
L1-L2	inferior	6	3
L2-L3	inferior	10	5
L3-L4	superior	8	4
L3-L4	inferior	4	2
L4-L5	inferior	4	2
L5-S1	superior	4	2
L5-S1	inferior	4	2

Table 2. Comparison of compositional traits between CEP subgroups.

	376 Da		4,000 Da		
	Static (n = 13)	Dynamic (n = 13)	Static (n = 10)	Dynamic (n = 10)	ANOVA p-value
Porosity	0.652 ± 0.081	0.660 ± 0.061	0.638 ± 0.061	0.638 ± 0.076	0.847
Hydration (mg water / mg dry wt)	1.605 ± 0.441	1.666 ± 0.404	1.585 ± 0.370	1.599 ± 0.437	0.965
s-GAG (μg / mg dry wt)	104.0 ± 17.75	100.9 ± 22.30	103.6 ± 45.11	103.6 ± 42.01	0.995
Collagen (μg / mg dry wt)	692.6 ± 156.3	701.8 ± 167.2	659.9 ± 174.4	665.0 ± 208.3	0.930
Thickness (mm)	0.800 ± 0.414 *	0.821 ± 0.401*	0.499 ± 0.130	0.503 ± 0.186	0.023

* $p < 0.05$ for 376 Da *vs.* 4,000 Da by post-hoc test.

Table 3. Associations (Pearson's correlation coefficient, r) between CEP compositional traits and transport enhancement values for a given solute size.

	Porosity	Hydration	*s*-GAG	Collagen	Thickness
376 Da Transport Enhancement	-0.910 α	-0.905 α	-0.601 β	-0.054	-0.311
4,000 Da Transport Enhancement	-0.939 α	-0.865 β	-0.138	0.086	0.201

α $p < 0.0001$, β $p < 0.01$